SciMedCentral

Annals of Clinical Pathology

Research Article

Therapeutic Potential of Arsenic Trioxide (ATO) in Treatment of Hepatocellular Carcinoma: Role of Oxidative Stress in ATO-Induced Apoptosis

Erika B. Dugo[1], Clement G. Yedjou[1,2], Jacqueline J. Stevens[1,2], and Paul B. Tchounwou[1]*

[1]*National Institutes of Health RCMI-Center for Environmental Health, Jackson State University, USA*

[2]*Department of Biology, College of Science, Engineering and Technology, Jackson State University, USA*

***Corresponding author**

Paul B. Tchounwou, National Institutes of Health RCMI-Center for Environmental Health, Jackson State University, 1400 Lynch Street, Box 18540, Jackson, MS 39217, USA, Tel: 1-601-979-0777; Fax: 1-601-979-0570; Email: paul.b.tchounwou@jsums.edu

Submitted: 31 October 2016

Accepted: 28 December 2016

Published: 04 January 2017

ISSN: 2373-9282

Keywords

- ATO
- Oxidative stress
- Apoptosis
- DNA fragmentation
- HepG$_2$ cells

Abstract

Hepatocellular carcinoma (HCC), the dominant form of primary liver cancer, is the sixth most common cancer in the world with more than 700,000 people diagnosed annually. Arsenic trioxide (ATO) has been shown to be a potent anticancer agent in various carcinomas, proving particularly effective in the clinical treatment of relapsed and refractory acute promyelocytic leukemia. However, its bioactivity and molecular mechanisms against HCC has not been fully studied. Using human HCC (HepG2) cells as a test model, we studied the effects of ATO and examined the role of oxidative stress (OS) and apoptosis in cytotoxicity. OS biomarkers showed a significant increase ($p< 0.05$) of malondialdehyde concentrations, and a gradual decrease of antioxidant enzymes (GPx & CAT) activities with increasing ATO doses. Flow cytometry data showed a dose dependent increase in annex in V positive cells and caspase 3 activities. These results were confirmed by data of the DNA laddering assay showing a clear evidence of nucleosomal DNA fragmentation, as well as data from Western blotting showing a significant modulation of specific apoptotic related proteins, including the activation of p53 and p21 expression and the down-regulation of Bcl-2 expression in ATO-treated cells. Taken together, our research demonstrates that ATO has a potential therapeutic effect against HCC, and its cytotoxicity may be mediated via oxidative stress and activation of the mitochondrial or intrinsic pathway of apoptosis.

ABBREVIATIONS

ANOVA: One Way Analysis of Variance; APL: Acute Promyelocytic Leukemia; APS: Ammonium Persulfate; ATCC: American Type Culture Collection; ATO: Arsenic Trioxide; ATRA: All Trans Retinoic Acid; BHT: Butylated Hydroxytoluene; CAT: Catalase; DMEM: Dulbecco's Modified Eagle's Medium; DMSO: Dimethylsulfoxide; DNA: Deoxyribonucleic Acid; DTT: Dithiothreitol; EDTA: Ethylene Diamine Tetraacetic Acid; FACS: Fluorescence Activated Cell Sorting System; FITC: Fluorescein Isothiocyanate; GST: Glutathione Transferase; Gpx: Glutathione Peroxidase; HCC: Hepatocellular Carcinoma; Hcl: Hydrochloric Acid; MDA: Malondialdehyde; MTT: 3-(4,5-Dimethyl-2-Thiazolyl)-2,5-Diphenyl-2tetrazoliumbromide; PE: Phycoerythrin; PBS: Phosphate Buffer Saline; PI: Propidium Iodine; ROS: Reactive Oxygen Species; SDS-PAGE: Sodium Dodecyl Sulfate Polyacrylamide Gel Electrophoris; SOD: Superoxide Dismutase; TBE: Tris-Borate EDTA; TEMED: Tetramethylethylenediamine; UV/Vis: Ultraviolet Visible Spectroscopy.

INTRODUCTION

Hepatocellular carcinoma is the dominant form of primary liver cancer occurring in patients with chronic liver disease and cirrhosis. Compared to all cancer sites, liver cancer death rates and incidence rates have increased among both men and women. Primary liver cancer is the sixth most common cancer in the world and the second leading cause of cancer death in men [1,2]. Over 700,000 people are diagnosed with liver cancer annually. Men are twice as likely as women to be diagnosed with liver cancer and the risk tends to increase with age. Liver cancer incidence has more than tripled since 1980 with rates increasing by 2.7% annually from 2003-2012 [3]. According to 2012 U.S. statistics

from the Center for Disease Control (CDC), Asian/Pacific Islander men had the highest liver cancer incidence rates followed by Hispanic and African American men [4].

Therapeutic treatment methods for hepatocellular carcinoma are determined by factors such as liver function, nodule quantity and size, age, presence of comorbidities and tumor extension. Presently, there are five treatment options for hepatocellular carcinoma but none have been shown to be a cure-all with regard to recurrence, patient survival and longevity [5]. Surgical treatments include resection or liver transplantation, but the best option between both depends on hepatic function and whether or not the patients have cirrhosis. Percutaneous ablation techniques include percutaneous ethanol injection and radiofrequency ablation which is most suitable for patients who have early stage hepatocellular carcinoma but are not candidates for resection or liver transplantation. Chemo embolization treatment is recommended for patients with intermediate stage, inoperable hepatocellular carcinoma whose liver function is preserved and has asymptomatic multinodular tumors that have not spread or invaded areas or vessels outside the liver. Radio embolization treatment is used in patients who are between intermediate and advanced stage hepatocellular carcinoma and are not suited for resection, liver transplantation or ablation [6,7]. Until 2007, there was no systemic treatment option for patients with advanced hepatocellular carcinoma. So far, sorafenib is the only systemic drug showing improved survival benefit in liver cancer patients [8-10]. However, better understanding of the mechanisms involved in hepatocellular carcinoma could lead to more novel therapeutic interventions. Our lab is focusing on the use of arsenic trioxide (ATO) as a possible therapeutic option for the treatment of hepatocellular carcinoma.

Recent reports by our laboratory show that oxidative stress and DNA damage play a key role in arsenic trioxide (ATO)-induced cytotoxicity in acute promyelocytic leukemia (HL-60) cells [11]. The premise for the present study is to further investigate the role of oxidative stress and apoptosis in ATO toxicity utilizing human hepatocellular carcinoma ($HepG_2$) cells as a model. Lipid peroxidation occurs as cells are being stressed by reactive oxygen species leading to loss of membrane function and integrity [12], thereby causing oxidative stress damage. Oxidative stress mediates many nocent effects of metals. The overproduction of reactive oxygen species (ROS) results in a significant increase in intracellular ROS, which leads to cellular damage, including lipid peroxidation, oxidative DNA modifications, protein oxidation and enzyme inactivation [13,14]. The imbalance between free radical generation and antioxidant defense systems resulting from oxidative stress is usually maintained in mammalian cells by key enzymes such as, superoxide dismutase (SOD), catalase (CAT), glutathione transferase (GST), glutathione peroxidase (GPx) and HO-1 that regulate intracellular ROS levels [15-17].

The apoptotic effect of ATO has been directly ascribed to oxidative stress or reactive oxygen species formation and the regulation of the mitochondrial pathway of apoptosis [18-20]. Initial stages of apoptosis are characterized by initiator caspase activation, alterations in the cellular redox potential, cell shrinkage, loss of membrane lipid asymmetry and chromatin condensation. Later stages associated with the execution phase of apoptosis are characterized by activation of execution caspases and endonucleases, apoptotic body formation and cell fragmentation [21,22]. Arsenic has been shown to increase the activities of caspases-3, -8 and -9, to suppress Bcl-2 expression, to increase p53 and p21 activity, to activate MAPKs (p-JNK and p38) and release cytochrome c, leading subsequently to apoptosis in several cell lines [23-28].

Few studies have reported that ATO may be a potential therapeutic agent for the treatment of liver cancer. Using MHCC97-H hepatocellular carcinoma cell line, Cui et al, [29], reported that ATO negatively affects HCC tumorigenesis through down regulation of B7-H4 protein expression and inhibition of JNK pathway. In a study with $HepG_2$ cells, Jiang et al, [30], demonstrated the ATO induces oxidative stress and apoptosis. Using TUNNEL and DNA laddering assays Yu et al, [31], reported that ATO-induced apoptosis is dose-dependent and is associated with the degradation of PML protein in the nuclei of in $HepG_2$ cells. Other studies have reported that ATO inhibits HCC cell migration and invasion through upregulation of mRNA-491 via a demethylation that blocks NFkB activation/signaling [32,33]. Meng et al, [34], also demonstrated that ATO alters miRNA expression profile in $HepG_2$ cells, and miRNA-29a seems to play an important role in ATO therapy against liver cancer. ATO has also been found to induce inhibition of metastatic potential of mouse hepatoma H22 cells [35]. The current study was designed to further examine the molecular mechanisms of ATO toxicity and its potential application for treatment of liver cancer.

It has been pointed out that the therapeutic potential of ATO against HHC may be enhanced by pharmaceutical products such as metformin [36], shikonin [37], survavin T34A [38], oridonin [39], genistein [40], and icari in [41]. On the other hand, it has been reported that the anti-cancer effect of sorafenib which is used for the treatment of HHC, is potentiated by ATO through the inhibition of Akt activation [42].

MATERIALS AND METHODS

Chemicals and culture media

Arsenic trioxide (ATO) with an active ingredient of 100% (w/v) arsenic in 10% nitric acid was purchased from Fisher Scientific in Houston, TX. Dulbecco's Modified Eagle's Medium (DMEM)-F12, G418, fetal bovine serum (FBS), and phosphate buffered saline (PBS) were purchased from American Type Culture Collection (ATCC) in Manassas, VA. Penicillin-Streptomycin was purchased from Gibco Invitrogen in Carlsbad, CA.

Cell culture and ATO treatment

The established human hepatocellular carcinoma cell line used in the study were $HepG_2$ (ATCC CRL-11997) cells purchased from ATCC in Manassas, VA. The $HepG_2$ cells were grown in 50 cm^2 tissue culture flasks in Dulbeco's Modified Eagle's Medium (DMEM) supplemented with 10% fetal bovine serum (FBS), 1% penicillin and streptomycin and 0.4mg/mL G418 at 37°C in a 5% CO_2 incubator until confluent. The cells were then trypsinized with 0.25% trypsin-0.03% EDTA, diluted, counted, and seeded at $5x10^6$ cells for each concentration of ATO (0.5, 1, 2, 4, and 8 µg/mL) for 24 hours at 37°C in a 5% CO_2 incubator.

Lipid peroxidation assay

The concentration of MDA was measured using a lipid peroxidation assay kit from Oxford Biomedical Research in Oxford, MI. The $HepG_2$ cells were treated with and without ATO according to the aforementioned concentrations for 24 hours. The cell suspensions were collected in 15 mL tubes, followed by low speed centrifugation. The cell pellets were resuspended in 0.5 mL Tris-HCl, pH 7.5 and lysed in the presence of 10µL Butylated hydroxytoluene (BHT) by the freeze-thaw method. The protein concentrations of the cell suspension were determined using the BioRad Dc Protein Assay kit from BioRad Hercules, CA [43]. A 200µL aliquot of the culture medium or 2mg of cell lysate protein were assayed for MDA utilizing the lipid peroxidation assay protocol as previously described [44,45]. The absorbance was measured at 586 nm and the concentration of MDA determined from the standard curve.

Glutathione peroxidase assay

Glutathione Peroxidase (GPx) activity was measured using a glutathione peroxidase assay kit from Calbiochem-EMD Biosciences in Gibbstown, NJ. The $HepG_2$ cells were treated with and without ATO according to the aforementioned concentrations for 24 hours. The cells were then isolated by cell scraping, rinsed twice with PBS and digested in 1mL of ice cold 50mM Tris-HCl, 5mM EthylenediamineTetraacetate (EDTA) and 1mM DTT. Cellular debris was removed by centrifugation and lysate used to determine GPx activity by following the protocol previously described [46,47] with a few modifications. The absorbance was measured at 340 nm using the Lab systems Multiskan Ascent microplate reader. Rate of the reaction was determined by constructing a standard curve as a function of absorbance versus time, and the GPx activity was expressed as nmol/minute/mL.

Catalase assay

Catalase activity was measured using a catalase assay kit from Calbiochem-EMD Biosciences in Gibbstown, NJ. The $HepG_2$ cells were treated with and without ATO according to the aforementioned concentrations for 24 hours. The cells were detached by cell scraping, rinsed twice with PBS and digested in 1mL of ice cold homogenization buffer (50mM potassium phosphate and 1mM EDTA). Cellular debris was removed by centrifugation and lysate used to determine catalase activity following the protocol described [48] with a few modifications. Measurement of catalase activity was based on the reaction of the enzyme with methanol in the presence of an optimal concentration of H_2O_2. The formaldehyde produced was measured spectrophotometrically at 540 nm using the Lab systems Multiskan Ascent microplate reader. One unit of catalase was defined as the formation of 1n mol of formaldehyde per minute per milliliter.

Annexin V/PI assay

$HepG_2$ cells were treated with and without ATO according to the aforementioned concentrations for 24 hours. Following treatment, the cells were isolated by trypsinization and rinsed twice with ice-cold PBS. Detection of phosphatidylserine on the outer leaflet of apoptotic cells was performed using Annexin V-FITC Apoptosis Detection kit in combination with propidium iodide (PI) staining (BD Pharmigen, Indianapolis, IN) according to the manufacturer's recommendations [49,50]. The samples were pelleted and resuspended in binding buffer at 1 X 10^6 cells/mL. Tubes were labeled for each sample with 5 µL of Annexin V FITC, 5 µL of dissolved PI and 100 µL of the cell suspension (100,000 cells) being added to each tube. Each sample was examined by flow cytometry using a FAC Sort (Becton Dickinson Co, San Diego, CA, USA). The percentages of apoptotic cells were determined by analysis of the dot plots using Cell Quest software.

Caspase-3 assay

$HepG_2$ cells were treated with and without ATO according to the aforementioned concentrations for 24 hours. Following treatment, the cells were isolated by trypsinization and rinsed twice with PBS. Active form of caspase-3 was determined by flow cytometry as previously described [51,52]. Cells (5×10^5) were washed, then fixed and permeabilized using the Cytofix/CytopermTM kit (BD Pharmingen) for 20 min at room temperature. Cells were washed with Perm/WashTM buffer, then stained with phycoerythrin (PE)-conjugated anti-active caspase-3 monoclonal antibodies using 20µL/1×10^6 cells for 60 min at room temperature in the dark. Following incubation with the antibody, cells were washed in Perm/Wash TM buffer, re-suspended in Perm/Wash TM buffer and analyzed using a FAC Sort (Becton Dickinson Co., San Diego, CA, USA) flow cytometer.

DNA laddering

$HepG_2$ cells were treated with and without ATO according to the aforementioned concentrations for 24 hours. The apoptotic DNA ladder kit was purchased from Roche Diagnostics Corporation (Indianapolis, IN). 2 x 10^6 cells were washed in PBS. The cells were then re-suspended in 200µL PBS and lysed in 200µL binding buffer. Centrifugation was used to separate the DNA in the lysate (which binds to the glass fiber fleece) from unbound lysate components (which flow through the fleece into a collection tube) as previously described [53]. The bound DNA was washed twice and eluted from the filter tube by centrifugation into 1.5 mL microcentrifuge tubes. An aliquot of each sample was taken to measure the optimal density at wavelength 280nm on the 2800 UV/VIS Spectrophotometer to determine the amount of DNA lysate to be loaded on the agarose gel. Twenty µg of the eluted DNA samples, 15 µL DNA Molecular Weight Marker and 15 µL Camptothecin-treated positive control cells were mixed with loading buffer and applied to a 1% agarose gel. The gel was then electrophoresed in TBE (Tris-borate EDTA) buffer at 40 V. The gel was stained using ethidium bromide (Sigma) for 15 minutes and the DNA ladder pattern on the gel visualized on the Typhoon 9400 Scanner.

Western blot analysis of specific ellular proteins

$HepG_2$ cells were treated with and without ATO according to the aforementioned concentrations for 24 hours. Protein lysate was prepared in lysis buffer and the protein concentration determined using the Bio Rad Dc Protein Assay kit (Hercules, CA). Western blot analysis was performed as previously described [54]. Samples with equal amount of protein was separated by SDS-PAGE with 4% stacking gel (2.4ml of distilled water, 1.8mL 4X upper gel buffer (1.5M Tris-Cl), 3.13mL of

30% acrylamide (BioRad), 75 µ l of 10% SDS, 37.5µ l of 10% (w/v) ammonium persulfate (APS) and 2.5µl of N,N,N′,N′-tetramethylethylenediamine) and 12% resolving gel (4.8ml of distilled water, 1.15ml of 30% acrylamide, 2ml of 4X lower gel buffer (0.5M Tris-Cl), 40µl of APS and 9.3µl of TEMED) running gel. The proteins were then transferred to a nitrocellulose membrane by semi-dry transfer system (BioRad). After blocking the non-specific space of the membrane with 10% non-fat milk in PBS-T (PBS with 0.5% Tween 20), the membranes were incubated with monoclonal antibodies (1:1000) against p53, p21, Bcl-2 and cytochrome c overnight at 4°C. The membranes were washed three times at 5-minute intervals with PBS-T, and incubated with horseradish peroxidase-conjugated secondary antibodies (1:10,000) for 1 hour at 4°C. The membranes were then washed five times at 10 minute intervals with PBS-T. Proteins were detected using enhanced chemiluminescence (ECL) detection reagents (Pierce Thermo Scientific). Relative band intensity was quantified using the Molecular Imager Gel Doc XR+ System and Image Lab Software Version 3.0 (Bio-Rad).

Statistical analysis

Statistical analysis was done using one way analysis of variance (ANOVA) for multiple samples and Student's t-test for testing differences. The results were represented as means ± standard deviations. All p-values less than 0.05 were considered to be significant. Oxidative stress and apoptotic data were presented graphically in the form of histograms, using Microsoft Excel computer program to represent the dose-response relationship among the treatment groups.

RESULTS

Induction of lipid peroxidation in ATO-treated Hepg$_2$ Cells

To elucidate the possible involvement of lipid peroxidation products in ATO induced toxicity, we performed the lipid peroxidation assay. The malondialdehyde (MDA) standard curve presented in Figure (1) shows a strong positive correlation with an r^2 value of 0.9983, with data on the effect of ATO on MDA production in HepG$_2$ cells presented in Figure (2). Upon 24 hours treatment with ATO, the MDA values were 1.55 ± 0.212, 4.75 ± 0.318, 7.25 ± 0.141, 9.15 ± 0.459, 10.6 ± 0.282, and 12.2 ± 0.106 µM in 0, 0.5, 1, 2, 4, and 8 µg/mL of ATO, respectively.

Induction of glutathione peroxidase in ATO-treated HepG$_2$ Cells

In this assay, glutathione peroxidase activity was determined for each sample by taking the absorbance reading at one minute time intervals over five minutes. Figure (3) demonstrates the effect of ATO on glutathione peroxidase activity in HepG$_2$ cells which revealed a dose dependent decrease in glutathione peroxidase activity with increasing ATO concentrations. There was a significant difference between the control and the treatment groups.

Induction of Catalase in ATO-treated HepG$_2$ Cells

In the catalase assay, the standard curve data showing a strong positive correlation and r^2 value of 0.9845 for formaldehyde concentration in Figure(4) was used to determine the catalase activity for HepG$_2$ cells exposed to each ATO concentration. Figure (5) demonstrates the effect of ATO on catalase activity revealing a slight elevation in catalase activity at low level of ATO treatment. When cells were treated with ATO levels of 2 µg/mL and higher, catalase activity decreased in a concentration dependent manner with the highest concentration (8 µg/mL) being significantly different (p< 0.05) compared to the control.

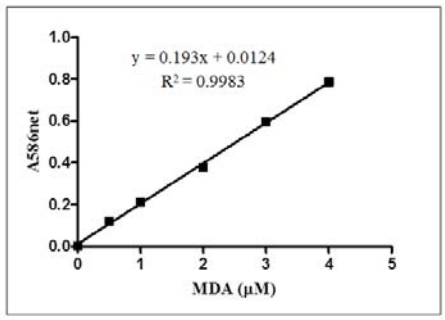

Figure 1 MDA standard curve with the absorbance wavelength of 586 nm on the y-axis and the control and different concentrations of MDA expressed in micromolar (µM) on the x-axis. R2 = 0.998.

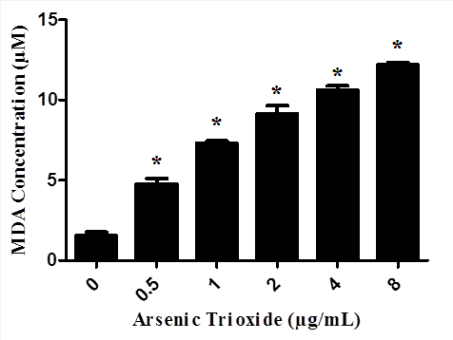

Figure 2 Effects of different concentrations of arsenic trioxide on MDA production in HepG2 cells treated for 24 hours. Data are representative of 3 independent experiments. * signifies data that are significantly different (p< 0.05) compared to the control by ANOVA.

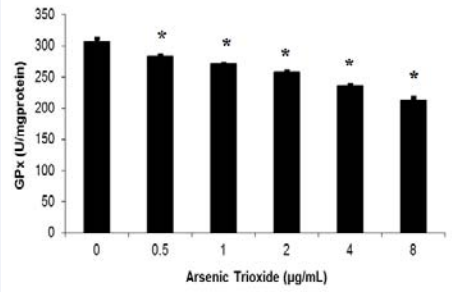

Figure 3 Effect of various concentrations of arsenic trioxide on glutathione peroxidase activity in HepG2 cells treated for 24 hours. Concentrations found to be significantly different (p<0.05) compared to the control are denoted by (*) according to ANOVA Dunnett.

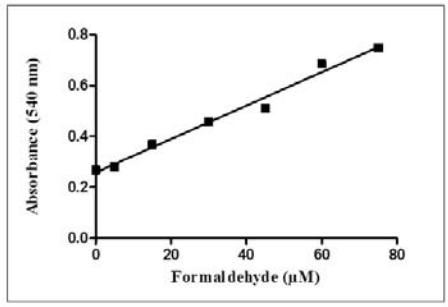

Figure 4 Formaldehyde standard curve showing absorbance values at 540 nm as a function of Formaldehyde concentration in µM.

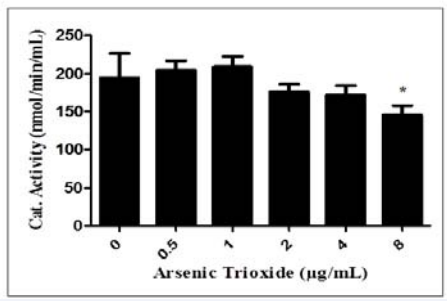

Figure 5 Effect of various concentrations of arsenic trioxide on catalase activity in HepG2 cells treated for 24 hours. Concentrations found to be significantly different ($p<0.05$) compared to the control is denoted by (*) according to ANOVA Dunnett.

Modulation of phosphatidylserine externalization by ATO in Hepg$_2$ Cells

Flow cytometric analysis was performed to determine the effect of ATO on early apoptosis utilizing the Annexin V/PI assay. Representative histograms are shown in Figure (6). Upon 24 hours of treatment, the results of the annexin V/PI staining showed that the percentages of early apoptotic cells (Annexin V positive cells) were 0.2 %, 1.6 %, 1.4 %, 21.4 %, 44.7 %, and 51.7 % in 0, 0.5, 1, 2, 4, and 8 µg/mL ATO in HepG$_2$ cells, respectively. The percentages of viable cells were 99.4 %, 93.5 %, 84.9 %, 76.5 %, 52.7 % and 46.7 %, respectively. The lower left quadrant of the histogram represents the viable cells which are Annexin V negative and PI negative. The lower right quadrant of the histogram represents the early apoptotic cells which are Annexin V positive and PI negative. Figure (7) shows a significant ($p< 0.05$) gradual increase in Annexin V positive cells at doses between 1-8 µg/ml ATO in HepG$_2$ cells compared to the control cells; indicative of a dose-dependent induction of apoptosis by ATO.

Activation of caspase-3 in ATO-treated Hepg$_2$ Cells

Flow cytometry data from the PE Caspase 3 assay was used to determine whether ATO contributed to late apoptosis in HepG$_2$ cells. Apoptosis is felt to be one of the key pathways of ATO mediated control of cancer cell growth in both solid tumors and leukemia. Loss of mitochondrial membrane potential, with subsequent increase in mitochondrial permeability, and

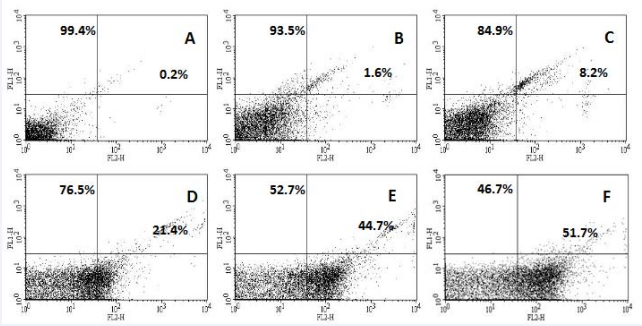

Figure 6 Representative flow cytometry analysis data from Annexin V/PI assay of HepG2 cells following 24h exposure. A, control; B, 0.5 µg/mL ATO; C, 1 µg/mL ATO; D, 2 µg/mL ATO; E, 4 µg/mL ATO; F, 8 µg/mL.

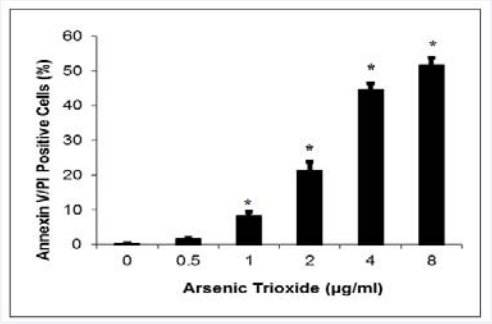

Figure 7 Induction of phosphatidylserine externalization by ATO in HepG2 cells. Percentage of Annexin V positive ATO-treated HepG2 cells undergoing early apoptosis following 24h exposure. * indicates significant difference ($p<0.05$) from the control, as well as, exposure time according to the ANOVA Dunnett's test.

activation of caspases by ATO contributes to the central trigger of the apoptotic processes [55-57]. Data in Figure (8) shows a dose dependent increase in Caspase 3 activity and ATO treatment. Figure (9) shows that the percentages of cells undergoing late apoptosis (Caspase 3 positive cells) were 4.5%, 9.8%, 14.5%, 16.6 %, 23.2%, and 31.1% in 0, 0.5, 1, 2, 4, and 8 µg/mL ATO in HepG$_2$ cells following 24h exposure, respectively. Significant differences ($p< 0.05$) in the number of apoptotic (Caspase-3 positive) cells were observed between the ATO-treated HepG$_2$ cells and the control cells.

Nucleosomal DNA fragmentation in ATO-treated HepG$_2$ cells

One of the characteristics of apoptosis is nucleosomal DNA fragmentation. To further study the action mechanism of ATO-induced apoptosis, DNA fragmentation assay by agarose gel electrophoresis was performed. Our results showed a typical ladder pattern and induction of nucleosomal DNA fragmentation in HepG$_2$ cells treated with ATO as presented in Figure (10).

Expression of Apoptotic-related genes in ATO-treated Hepg$_2$ Cells

Western blot analysis was conducted to determine the

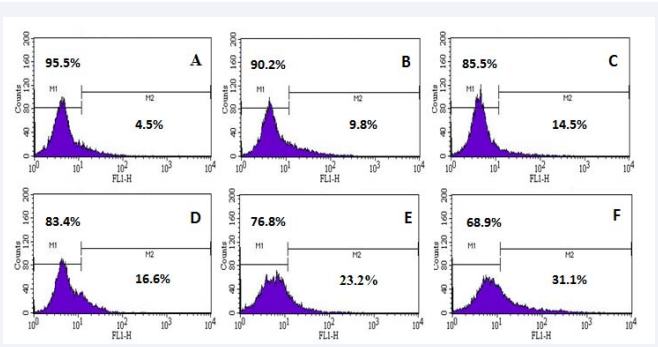

Figure 8 Representative flow cytometry analysis data from Caspase 3 assay in HepG2 cells following 24h exposure.A, control; B, 0.5 µg/mL ATO; C, 1 µg/mL ATO; D, 2 µg/mL ATO; E, 4 µg/mL ATO; F, 8 µg/mL.

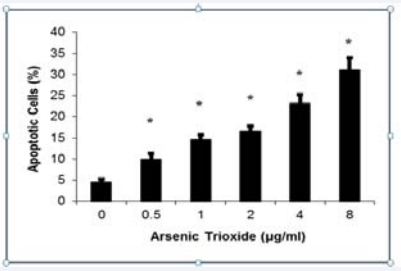

Figure 9 Activation of Caspase-3 by ATO in HepG2 cells. Percentage of late apoptotic ATO-treated HepG2 cells following 24h exposure utilizing Caspase-3 analysis. * indicates significant difference ($p<0.05$) from the control according to the ANOVA Dunnett's test.

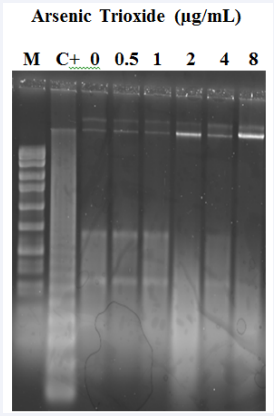

Figure 10 DNA fragmentation by agarose gel electrophoresis. HepG2 cells were treated with various concentrations of ATO for 24h. Lane 1: DNA molecular weight marker (M); Lane 2: Positive control (C+) cells were induced for apoptosis by camptothecin; Lane 3: Control or untreated HepG2 cells; Lanes 4, 5, 6, 7, 8 and 9: HepG2 cells treated with 0.5, 1, 2, 4, 8, and 16 µg/mL of arsenic trioxide.

expression of specific cellular proteins in hepatocellular carcinoma $HepG_2$ cells treated with ATO. Data represented in Figure (11) shows the expression of apoptotic-related genes p53, p21, Bcl-2 and cytochrome c. In our study, densitometric analysis of p53 and p21 showed increased expression in ATO-treated $HepG_2$ cells compared to control with p53 expression being significantly different in all ATO concentrations (Figure 12) and p21 expression being significantly different between 2-8 µg/ml ATO concentrations (Figure 13). Densitometric analysis of Bcl-2 showed that expression was reduced in ATO-treated $HepG_2$ cells with significant ($p< 0.05$) down regulation at 0.5, 4 and 8 µg/ml ATO concentrations (Figure 14). Densitometric analysis showed an increase in cytochrome c expression in a dose dependent manner with ATO concentrations between 0.5-8 µg/ml being significantly ($p< 0.05$) different compared to the control (Figure 14).

DISCUSSION

Apoptosis or programmed cell death plays an important role in the physiological process and homeostasis of the cell [58].

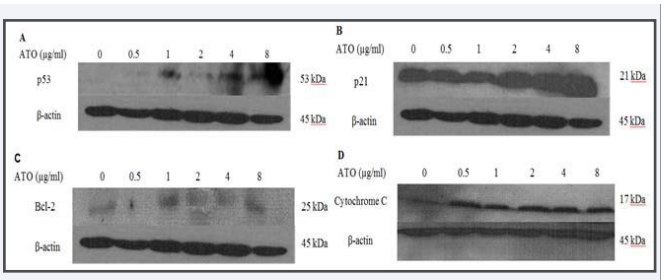

Figure 11 Western blot analysis of apoptotic protein expression (A-D) in 24h ATO-treated HepG2 cells. A – p53; B – p21; C – Bcl-2 and D – cytochrome c.

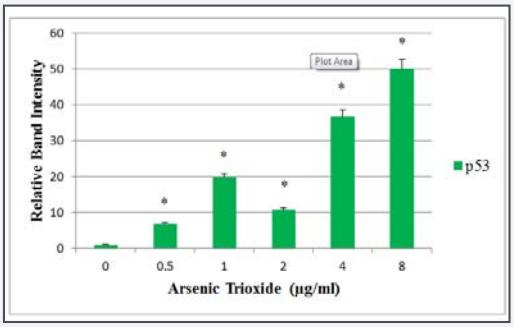

Figure 12 Densitometric analysis of p53 expression in 24h ATO-treated HepG2 cells.

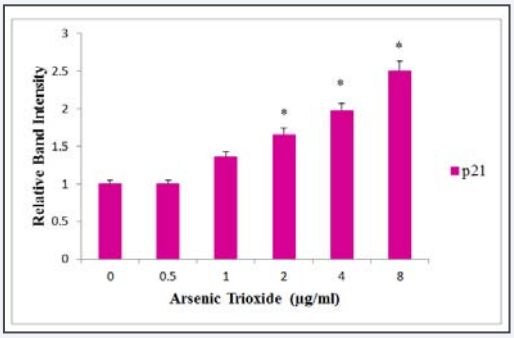

Figure 13 Densitometric analysis of p21 expression in 24h ATO-treated HepG2 cells.

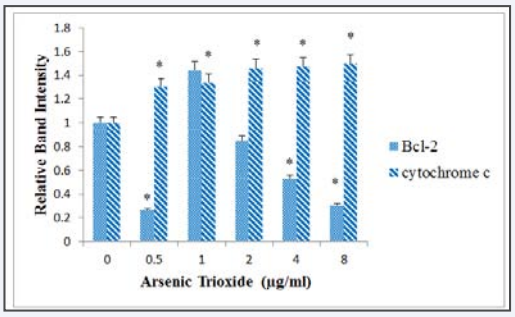

Figure 14 Densitometric analysis of Bcl-2 and cytochrome c expression in 24h ATO-treated HepG2 cells.

Apoptosis is a highly organized process characterized by the progressive activation of precise pathways leading to specific biochemical and morphological alterations [59]. Recent studies in our laboratory indicate that ATO induces apoptosis in HL-60 and A549 cells [60,61]. The present study focuses on the role oxidative stress plays in arsenic-induced apoptosis in human hepatocellular carcinoma ($HepG_2$) cells. Oxidative stress is an imbalance between the production and disposal of reactive oxygen which forms as a result of free radical formation capable of initiating lipid peroxidation and alterations in the antioxidant cellular defense system. The antioxidant response is one of the most efficient mechanisms of cell defense where superoxide dismutase (SOD), catalase (CAT), glutathione transferase (GST), glutathione peroxidase (GPx) and HO-1 are among the main enzymatic mechanisms involved in clearing and scavenging ROS to maintain low intracellular levels [62,63]. Data from our lipid peroxidation assay as seen in Figure (2) show that arsenic trioxide significantly increases ($p< 0.05$) malondialdehyde (MDA) levels in human hepatocellular carcinoma ($HepG_2$) cells in a dose-dependent manner. In addition when we looked at whether the detoxification systems and antioxidants were compromised, we found that ATO significantly decreases glutathione peroxidase activities with increasing ATO concentrations in $HepG_2$ cells and results in a non-linear decrease of catalase activities with 8µg/ml ATO being the most significant (Figures 3 and 5). When comparing glutathione peroxidase and catalase activity in ATO-treated $HepG_2$ cells, catalase activity was found to be higher, suggesting that it is a stronger scavenger for the decomposition of H_2O_2, one of the main ROS involved in arsenic-induced DNA damage [64,65]. Findings consistent with previous data suggesting that alteration of oxidative stress markers is due to overuse/failure of the antioxidant defense system secondary to reactive oxygen species production [66].

Mitochondria are an important organelle involved in arsenic-induced apoptosis [67,68]. There are two major pathways of apoptosis, the death receptor pathway (extrinsic) and the mitochondrial pathway (intrinsic) [69]. The mitochondrial pathway of apoptosis can be triggered by a variety of stimuli, including chemotherapeutic agents, UV radiation, and oxidative stress. One of the early events in apoptotic cell death is loss of asymmetry in the phospholipid bilayer of the plasma membrane with translocation of phosphatidylserine from the inner to the outer leaflet, which can be detected by increased binding of fluorescence tagged Annexin V to the external surface of the cells. As seen in Figures (6) and (7), data from the Annexin V-PI staining showed an increase in the percentage of cells in the bottom right quadrants of the dot plot with increasing ATO concentrations, indicative of apoptosis. Similar results have been seen in studies of keratinocytes, human leukemia cells and peripheral blood mononuclear cells [70-72]. Activation of caspases appears to be directly responsible for many of the molecular and structural changes in apoptosis. Depending on the stimulus that initiates apoptosis, different caspase cascades are activated [73]. Caspase-3 plays an essential role as an executor in apoptosis [74,75]. Figures (8) and (9) show the activation of caspase-3 as assessed by flow cytometry to have a dose-dependent increase in the percentage of cells undergoing late apoptosis. Our results indicate ATO-induced hepatocyte death occurring in vitro to be apoptotic and caspase-mediated, which is a common and critical component of the apoptotic cell death pathway. In a similar study, Jiang et al [30] reported that ATO induced apoptosis in $HepG_2$ cells is mediated via oxidative stress through the mitochondria pathway and activation of caspases.

One of the hallmarks of apoptosis is nucleosomal DNA fragmentation that occurs due to numerous events initiated by caspase 3 [76]. As seen in Figure (10), our results from the DNA fragmentation assay by agarose gel electrophoresis showed a typical ladder pattern in $HepG_2$ cells treated with ATO. Earlier studies reported that arsenite concentrations above 0.25 mM induced DNA strand breakage in human leukemia cells and Chinese hamster ovarian cells [77]. Arsenite also induced deletion, aneuploidy, sister chromatid exchange and different chromosomal aberrations [78-80]. The DNA ladder pattern obtained from our results is highly specific for apoptotic mode of cell death, thereby confirming arsenic induced cellular apoptosis.

Arsenic has been found to induce gene expression in a number of apoptotic and stress response proteins and transcription factors [81-83]. p53 is a tumor suppressor gene that regulates the expression of genes involved in growth arrest, DNA damage and apoptosis [84,85]. In our study, we demonstrated an upregulation of p53 expression with respect to increasing ATO concentrations in $HepG_2$ cells (Figures 11A and 12). Other studies also showed that p53 expression increased in response to ATO exposure in human leukemia cells, TM4 Sertoli cells and pancreatic cells [86-88]. Activation of p53 in our study may be a result of ROS generation, suggesting an important consequence of oxidant-induced activation of p53. Arsenic can induce, inhibit or have no influence on the p53 expression and its regulation of down-stream genes like p21 [89-91]. Arsenic has been reported to increase p21 expression in several cell lines revealing its role in the apoptotic signaling pathway [92-94]. The activation of p21 within a cell either helps to block cell cycle progression to allow time for DNA repair before replication or causes apoptosis via induction of the proapoptotic protein BAX and down regulation of the antiapoptotic protein Bcl-2 in heavily damaged cells [95,96]. Our results show a dose-dependent increase in p21 expression with respect to ATO exposure in $HepG_2$ cells (Figures 11B and 13). Earlier studies have reported up regulation of p21 to be time and dose-dependent in human pancreatic cancer cells and A498 renal carcinoma cells [97, 98]. The up regulation of p21 in our study may play a role in the stress response to ATO and may serve as an executioner of apoptosis following caspase activation.

Bcl-2 is an anti-apoptotic protein that acts to stabilize the mitochondrial membrane, control the mitochondrial membrane permeability to prevent the release of cytochrome C, and suppresses the activation of the caspase-3 apoptotic cascade. P53 antagonizes the antiapoptotic activities of Bcl-2, Bcl-xl and Mcl-1 thus, allowing proapoptoticBax, Bak and Bid to trigger apoptosis [99,100]. Translocation of p53 to the mitochondria induces apoptosis via cytochrome c release and activation of the intrinsic pathway which in turn is also regulated [101,102]. In our study, we examined the effect of arsenic trioxide on Bcl-2 expression in $HepG_2$ cells, and observed a biphasic response indicating an up-regulation at 1 µg/mL of ATO treatment followed by a significant dose-dependent down-regulation at higher doses of ATO exposure (Figures 11C and 14). The up regulation of Bcl-2 expression at lower level of exposure may be due to an arsenic-induced hormetic effect; a condition that has previously been characterized by a stimulation of cell proliferation or induction of mitogenic effect at low doses, followed by an inhibition of cell viability or induction of cytotoxicity at higher doses [60,103-105]. This adaptive or protective response at low doses is characteristic of many oxidative stress causing compounds including chemotherapeutic agents [106]. Between 1 and 8 µg/mL ATO, Bcl-2 expression was significantly down-regulated. Similar results have been found in gallbladder carcinoma cells and acute promyelocytic leukemia cells treated with ATO [107,108]. These results indicate that ATO exposure blocks Bcl-2 from preventing apoptosis in $HepG_2$ cells, thereby allowing cytochrome c to be released. Increased permeability of the mitochondrial membrane during apoptosis triggers the release of cytochrome c from mitochondria in the apoptotic process in response to proapoptotic stimuli. The release of cytochrome c into the cytoplasm activates caspases cascade [109-111]. Our results show an increase of cytochrome c expression in ATO-treated $HepG_2$ cells compared to the control (Figures 11D and 14). Previous studies reported a release of cytochrome c into the cytosol of ATO-treated mouse embryonic fibroblasts [112]. The release of cytochrome c into the cytoplasm results in caspase 9 activation and subsequent activation of caspase 3, ultimately leading to apoptosis as evidenced by data presented in this paper.

CONCLUSIONS

Our study demonstrates that arsenic trioxide is highly toxic to human hepatocellular ($HepG_2$) carcinoma cells resulting in oxidative stress and apoptosis. The generation of reactive oxygen species within the cell occurs as a result of oxidative stress. This statement is confirmed by the results from the lipid peroxidation assay showing an increase in MDA, as well as a decrease in the antioxidant enzyme activity of GPx and catalase in ATO-treated cells. In response to ROS, antioxidant defense enzymes are activated to metabolize these oxidants, however a higher level of ATO treatment, as indicated by our data, shows a loss of activation thus pointing to its inability to protect cells from oxidative stress. Flow cytometric analysis showed an increase of caspase 3 and annexin V activity with increasing ATO concentrations. Also, a characteristic DNA fragmentation was observed in the DNA laddering assay. Western blot analysis of ATO-treated $HepG_2$ cells revealed a down regulation of Bcl-2 expression, and an upregulation of cytochrome c, p53 and p21 expression. Taken together, these findings provide further insights into the role oxidative stress plays in ATO-induced apoptosis; making its potential use for the treatment of hepatocellular carcinoma worth exploring further.

ACKNOWLEDGEMENTS

PBT, CGY and EBD conceived, and designed the study. EBD performed the experiments and drafted the manuscript. CGY supervised the experiments and assisted in performing data interpretation. JJS provided critical review and manuscript editing. PBT participated in the implementation of the study and reviewed the manuscript for submission. All authors read and approved the final draft of the manuscript. This research was supported by a grant from the National Institutes of Health / National Institute on Minority Health and Health Disparities (G12MD007581) through the RCMI Center for Environmental Health at Jackson State University.

REFERENCES

1. Torre LA, Bray F, Siegel RL, Ferlay J, Lortet-Tieulent J, Jemal A. Global cancer statistics. CA Cancer J Clin. 2015; 65: 87-108.
2. Jemal A, Bray F, Center MM, Ferlay J, Ward E, Forman D. Global cancer statistics. CA Cancer J Clin. 2011; 61: 69-90.
3. American Cancer Society. Cancer Facts & Figures 2016. Atlanta, Ga: American Cancer Society. 2016.
4. U.S. Cancer Statistics Working Group. United States Cancer Statistics: 1999-2012 Incidence and Mortality Web-based Report. Atlanta: U.S. Department of Health and Human Services, Centers for Disease Control and Prevention and National Cancer Institute.
5. Pinter M, Trauner M, Peck-Radosavljevic M, Sieghart W. Cancer and liver cirrhosis: implications on prognosis and management. ESMO. 2016; 1-15.
6. Lencioni R, Crocetti L. Local-regional treatment of hepatocellular carcinoma. Radiology. 2012; 262: 43-58.
7. National Cancer Institute. Physician Data Query (PDQ). Adult Primary Liver Cancer Treatment. Retrieved 1 March 2016.
8. Llovet JM, Ricci S, Mazzaferro V, Hilgard P, Gane E, Blanc JF, et al. Sorafenib in advanced hepatocellular carcinoma. N Engl J Med. 2008; 359: 378-390.
9. Pascual S, Herrera I, Irurzun. New advances in hepatocellular carcinoma. World J Hepatol. 2016; 8: 421-438.
10. Ingle P, Samsudin S, Chan P, Ng M, Heng L, Yap S, Chai A, Wong A. Development and novel therapeutics in hepatocellular carcinoma: a review. Ther and Clin Risk Manag. 2016; 12: 445-455.
11. Kumar S, Yedjou CG, Tchounwou PB. Arsenic trioxide induces oxidative stress, DNA damage, and mitochondrial pathway of apoptosis in human leukemia (HL-60) cells. J Exp Clin Cancer Res. 2014; 33: 42-53.
12. Aust SD, Marehouse LA, Thomas CE. Role of metals in oxygen radical reactions. J Free Radic Biol Med. 1985; 1: 3-25.
13. Halliwell B, Gutteridge JMC. Oxygen toxicity, oxygen radicals, transition metals and disease. Biochem J. 1984; 219: 1-14.
14. Pelicano H, Feng L, Zhou Y, Carew JS, Hileman EO, Plunkett W, et al. Inhibition of Mitochondrial Respiration: A novel strategy to enhance drug-induced apoptosis in human leukemia cells by a reactive oxygen species-mediated mechanism. J Biol Chem. 2003; 278: 37832-37839.
15. Valko M, Leibfritz D, Moncol J, Cronin MT, Mazur M, Telser J. Free radicals and antioxidants in normal physiological functions and human disease. Int J Biochem Cell Biol. 2007; 39: 44-84.

16. Hirano S, Kobayashi Y, Cui X, Kanno S, Hayakawa T, Shraim A. The accumulation and toxicity of methylated arsenicals in endothelial cells: important roles of thiol compounds. Toxicol Appl Pharmacol. 2004; 198: 458-467.

17. Nesnow S, Roop BC, Lambert G, Kadiiska M, Masan RP, Cullen WR et al. DNA damage induced by methylated trivalent aresnicals is mediated by reactive oxygen species. Chem Res Toxicol. 2002; 15: 1627-1634.

18. Chen F, Vallyathan V, Castranova V, Shi X. Cell apoptosis induced by carcinogenic metals. Mol Cell Biochem. 2001; 222: 183-188.

19. Ramos AM, Fernandez C, Amran D, Sancho P, de Blas E, Aller P. Pharmacologic inhibitors of PI3K/Akt potentiate the apoptotic action of the antileukemic drug arsenic trioxide via glutathione depletion and increased peroxide accumulation in myeloid leukemia cells. Blood. 2005; 105: 4013-4020.

20. Ramos AM, Fernandez C, Amran D, Esteban D, de Blas E, Palacios MA, et al. Pharmacologic inhibitors of extracellular signal-regulated kinase (ERKs) and c-Jun NH(2)-terminal kinase (JNK) decrease glutathione content and sensitize human promonocytic leukemia cells to arsenic trioxide-induced apoptosis. J Cell Physiol. 2006; 209: 1006-1015.

21. Hengartner MO. The biochemistry of apoptosis. Nature. 2000; 407: 770-776.

22. Galluzzi L, Maiuri MC, Vitale I, Zischka H, Castedo M, Zitvogel L et al. Cell death modalities: classification and pathophysiological implication. Cell Death Differ. 2007; 14: 1237-1243.

23. Akao Y, Mizoguchi H, Kojima S, Naoe T, Ohishi N, Yagi K. Arsenic induces apoptosis in B-cell leukaemic cell lines in vitro: activation of caspases and down-regulation of Bcl-2 protein. Br J Haematol. 1998; 102: 1055-1060.

24. Huang C, Ma WY, Li J, Dong Z. Arsenic induces apoptosis through a c-Jun NH2-terminal kinase-dependent, p53-independent pathway. Cancer Res. 1999; 59: 3053-3058.

25. Choi YJ, Park JW, Suh SI, Mun KC, Bae JH, Song DK, et al. Arsenic trioxide-induced apoptosis in U937 cells involve generation of reactive oxygen species and inhibition of Akt. Int J Oncol. 2002; 21: 603-610.

26. Nakagawa Y, Akao Y, Morikawa H, Hirata I, Katsu K, Naoe T, et al. Arsenic trioxide-induced apoptosis through oxidative stress in cells of colon cancer cell lines. Life Sci. 2002; 70: 2253-2269.

27. Lee CH, Yu CL, Liao WT, Kao YH, Chai CY, Chen GS, et al. Effects and interactions of low doses of arsenic and UVB on keratinocyte apoptosis. Chem Res Toxicol. 2004; 17: 1199-1205.

28. Zheng Y, Shi Y, Tian C, Jiang C, Jin H, Chen J, et al. Essential role of the voltage-dependent anion channel (VDAC) in mitochondrial permeability transition pore opening and cytochrome c release induced by arsenic trioxide. Oncogene. 2004; 23: 1239-1247.

29. Cui L, Gao B, Cao Z, Chen X, Zhang S, Zhang W. Downregulation of B7-H4 in the MHCC97-H hepatocellular carcinoma cell line by arsenic trioxide. Mol Med Rep. 2016; 13: 2032-2038.

30. Jiang L, Wang L, Chen L, Cai GH, Ren QY, Chen JZ, et al. As2O3 induces apoptosis in human hepatocellular carcinoma HepG2 cells through a ROS-mediated mitochondrial pathway and activation of caspases. Int J ClinExp Med. 2015; 8: 2190-2196.

31. Yu D, Wang Z, Zhu L, Chew EC. Nuclear matrix associated protein PML: an arsenic trioxide apoptosis therapeutic target protein in HepG2 cells. Chin Med J (Engl). 2003; 116:93-98.

32. Jiang F, Wang X, Liu Q, Shen J, Li Z, Li Y, et al. Inhibition of TGF-β/SMAD3/NF-κB signaling by microRNA-491 is involved in arsenic trioxide-induced anti-angiogenesis in hepatocellular carcinoma cells. Toxicol Lett. 2014; 231:55-61.

33. Wang X, Jiang F, Mu J, Ye X, Si L, Ning S, et al. Arsenic trioxide attenuates the invasion potential of human liver cancer cells through the demethylation-activated microRNA-491. Toxicol Lett. 2014; 227: 75-83.

34. Meng XZ, Zheng TS, Chen X, Wang JB, Zhang WH, Pan SH, et al. microRNA expression alteration after arsenic trioxide treatment in HepG-2 cells. J Gastroenterol Hepatol. 2011; 6:186-193.

35. Zhao XS, Song PL, Sun B, Jiang HC, Liu TF. Arsenic trioxide inhibits metastatic potential of mouse hepatoma H22 cells in vitro and in vivo. Hepatobiliary Pancreat Dis Int. 2009; 8: 510-517.

36. Yang X, Sun D, Tian Y, Ling S, Wang L. Metformin sensitizes hepatocellular carcinoma to arsenic trioxide-induced apoptosis by downregulating Bcl2 expression. Tumour Biol. 2015; 36: 2957-2964.

37. Song J, Zhao Z, Fan X, Chen M, Cheng X, Zhang D, et al. Shikonin potentiates the effect of arsenic trioxide against human hepatocellular carcinoma in vitro and in vivo. Oncotarget. 2016; 12041.

38. Huang A, Yue D, Liao D, Cheng L, Ma J, Wei Y, et al. SurvivinT34A increases the therapeutic efficacy of arsenic trioxide in mouse hepatocellular carcinoma models. Oncol Rep. 2016; 36: 3283-3290.

39. Chen G, Wang K, Yang BY, Tang B, Chen JX, Hua ZC. Synergistic antitumor activity of oridonin and arsenic trioxide on hepatocellular carcinoma cells. Int J Oncol. 2012; 40: 139-147.

40. Ma Y, Wang J, Liu L, Zhu H, Chen X, Pan S, Sun X, Jiang H. Genistein potentiates the effect of arsenic trioxide against human hepatocellular carcinoma: role of Akt and nuclear factor-κB. Cancer Lett. 2011; 301: 75-84.

41. Li W, Wang M, Wang L, Ji S, Zhang J, Zhang C. Icariin synergizes with arsenic trioxide to suppress human hepatocellular carcinoma. Cell Biochem Biophys. 2014; 68: 427-436.

42. Zhai B, Jiang X, He C, Zhao D, Ma L, Xu L, et al. Arsenic trioxide potentiates the anti-cancer activities of sorafenib against hepatocellular carcinoma by inhibiting Akt activation. Tumour Biol. 2015; 36: 2323-2234.

43. Peterson GL. Review of the Folin Phenol Protein Quantitation Method of Lowry, Rosebrough, Farr, and Randall. Anal Biochem. 1979; 100: 201-220.

44. Esterbauer H, Schaur RJ, Zollner H. Chemistry and biochemistry of 4-hydroxynonenal, malonaldehyde and related aldehydes. Free Rad Biol Med. 1991; 11: 81-128.

45. Janero DR. Malondialdehyde and thiobarbituric acid activity as diagnostic indices of lipid peroxidation and peroxidatve tissue injury. Free Rad Biol Med. 1990; 9: 515-540.

46. Paglia E, Valentine WN. Studies on the quantitative and qualitative characterization of erythrocyte glutathione peroxidase. J Lab Cm Med. 1967; 70: 158-169.

47. Forstrom JW, Zakowski JJ, Tappel AL. Identification of the catalytic site of rat liver glutathione peroxidase as selenocysteine. Biochemistry. 1978; 17: 2639-2644.

48. Johansson LH, LA Håkan Borg. A spectrophotometric method for determination of catalase activity in all tissue samples. Anal Biochem. 1988; 174: 331-336.

49. Koopman G, Reutelingsperger CP, Kuijten GA, Keehnen RM, Pals ST, van Oers MH. Annexin V for flow cytometric detection of phosphatidylserine expression on B cells undergoing apoptosis. Blood. 1994; 84: 1415-1420.

50. Van Engeland M, Ramaekers FC, Schutte B, Reutelingsperger CP. A novel assay to measure loss of plasma membrane asymmetry during apoptosis of adherent cells in culture. Cytometry. 1996; 24: 131-139.

51. Fujita N, Tsuruo T. Involvement of Bcl-2 cleavage in the acceleration of VP-16-induced U937 cell apoptosis. Biochem Biophys Res Commun. 1998; 246: 484-488.

52. Belloc F, Belaud-Rotureau MA, Lavignolle V, Bascans E, Braz-Pereira E, Durrieu F, Lacombe F. Flow cytometry detection of caspase 3 activation in preapoptotic leukemic cells. Cytometry. 2000; 40:151.

53. Yeung MC. Accelerated apoptotic DNA laddering protocol. Biotechniques. 2002; 33: 734-736.

54. Towbin H, Staehelin T, Gordon J. Electrophoretic transfer of proteins from polyacrylamide gels to nitrocellulose sheets: procedure and some applications. Proc Natl Acad Sci USA. 1979; 76: 4350-4354.

55. Soignet SL, Maslak P, Whag ZG, Jhanwar S, Calleja E, Dardashti LJ. Complete remission after treatment of acute promyelocytic leukemia with arsenic trioxide. N Eng J Med. 1998; 339: 1341-1348.

56. Shao QS, Ye ZY, Ling ZQ, Ke JJ. Cell cycle arrest and apoptotic cell death in cultured human gastric carcinoma cells mediated by arsenic trioxide. World J Gastroenterol. 2005; 11: 3451-3456.

57. Charoensuk V, Gati WP, Weinfeld M, Le XC. Differential cytotoxic effects of arsenic compounds in human acute promyelocytic leukemia cells. Toxicol Appl Pharmacol. 2009; 239: 64-70.

58. Hengartner MO. The biochemistry of apoptosis. Nature (Lond.). 2000; 407: 770-776.

59. Liu L, Trimarchi JR, Navarro P, Blasco MA, Keefe DL. Oxidative stress contributes to arsenic-induced telomere attrition, chromosome instability, and apoptosis. J Biol Chem. 2003; 278: 31998-32004.

60. Yedjou CG, Tchounwou PB, Jenkins J, McMurray R. Basic Mechanisms of Arsenic Trioxide (ATO)-Induced Apoptosis in Human Leukemia (HL-60) Cells. J Hematol Oncol. 2010; 3: 28-37.

61. Walker AM, Stevens JJ, Ndebele K, Tchounwou PB. Arsenic Trioxide Modulates DNA Synthesis and Apoptosis in Lung Carcinoma Cells. Int J Environ Res Public Health. 2010; 7: 1996-2007.

62. Shi H, Shi X, Liu KJ. Oxidative mechanism of arsenic toxicity and carcinogenesis. Mol Cell Biochem. 2004; 255: 67-78.

63. Flora SJ. Arsenic-induced oxidative stress and its reversibility following combined administration of N-acetylcysteine and meso 2,3-dimercaptosuccinic acid in rats. Clin Exp Pharmacol and Physiol. 1999; 26: 865-874.

64. Inoue M. Protective mechanisms against reactive oxygen species. The liver: biology and pathology. Eds. IM Arias, JL Boyer, FV Chisari, N Fausto, D Schachter and DA Shafritz. 4th Edition. Philadelphia: Lippincott Williams & Wilkins. 2001; 19: 281-290.

65. Starke PE, Farber JL. Endogenous defense against the cytotoxicity of hydrogen peroxide in cultural hepatocytes. J Biol Chem. 1985; 260: 86-92.

66. Ryter SW, Kim HP, Hoetzel A, Park JW, Nakahira K, Wang X, et al. Mechanisms of cell death in oxidative stress. Antioxid Redox Signal. 2007; 9: 49-89.

67. Woo SH, Park IC, Park MJ, Lee HC, Lee SJ, Chun YJ, et al. Arsenic trioxide induces apoptosis through a reactive oxygen species-dependent pathway and loss of mitochondrial membrane potential in HeLa cells. Int J Oncol. 2002; 21: 57-63.

68. Guo J, JY Zhang. Investigation of apoptosis mechanism of arsenic trioxide on oral squamous cell carcinoma. Zhonghua Kou Qiang Yi XueZaZhi=Chinese Journal of Stomatology. 2003; 38: 20-23.

69. Grimm S, Brdiczka D. The permeability transition pore in cell death. Apoptosis. 2007; 12: 841-855.

70. Graham-Evans B, Cohly HP, Yu H, Tchounwou PB. Arsenic-induced genotoxic and cytotoxic effects in human keratinocytes, melanocytes and dendritic cells. Int J Environ Res Public Health. 2004; 1: 83-89.

71. Yedjou CG, Tchounwou PB. *In-vitro* cytotoxic and genotoxic effects of arsenic trioxide on human leukemia (HL-60) cells using the MTT and alkaline single cell gel electrophoresis (Comet) assays. Mol Cell Biochem. 2007; 301: 123-130.

72. Banerjee N, Banerjee M, Ganguly S, Bandyopadhyay S, Das JK, Bandyopadhay A, et al . Arsenic-induced mitochondrial instability leading to programmed cell death in the exposed individuals. Toxicology. 2008; 246: 101-111.

73. Rocha S, Soengas MS, Lowe SW, Glanzmann C, Fabbro D, Winterhalter K, et al. Protein kinase C inhibitor and irradiation-induced apoptosis: relevance of the cytochrome c-mediated caspase-9 death pathway. Cell Growth Differ. 2000; 11: 491-499.

74. Alnemri ES, Livingston DJ, Nicholson DW, Salvesen G, Thornberry NA, Wong WW, et al. Human ICE/CED-3 Protease Nomenclature. Cell. 1996; 87: 171.

75. Porter AG, Janicke RU. Emerging roles of caspase-3 in apoptosis. Cell Death Differ. 1999; 6: 99-104.

76. Enari M, Sakahira H, Yokoyama H, Okawa K, Iwamatsu A, S Nagata. A caspase-activated DNase that degrades DNA during apoptosis, and its inhibitor ICAD. Nature. 1998; 391: 43-50.

77. Wang SD, Holladay DC, Ahmed SA, Robertson JH. Reproductive and developmental toxicity of arsenic in rodents: a review. Int J Toxicol. 2006; 25: 319-331.

78. Gurr JR, Lin YC, Ho IC, Jan KJ, Lee TC. Induction of chromatid breaks and tetraploidy in Chinese hamster ovary cells by treatment with sodium arsenite during the G2 phase. Mutat Res. 1993; 319: 135-142.

79. Huang RN, Ho IC, Yih LH, Lee TC. Sodium arsenite induces chromosome endoreduplication and inhibits protein phosphatase activity in human fibroblasts. Environ Mol Mutagen. 1995; 25: 188-196.

80. Kochhar TS, Howard W, Hoffman S, Brammer-Carleton L. Effect of trivalent arsenic in causing chromosome alterations in cultured CHO cells. Toxicol Lett. 1996; 84: 37-42.

81. Parrish AR, Zheng KD, Turney XH, Younis HS, Gandolfi AJ. Enhanced transcription factor DNA binding and gene expression induced by arsenite or arsenate in renal slices. Toxicol Sci. 1999; 50: 98-105.

82. Yih LH, Peck K, Lee TC. Changes in gene expression profiles of human fibroblasts in response to sodium arsenite treatment. Carcinogenesis. 2002; 23: 867-876.

83. Tchounwou PB, Yedjou CG, Dorsey WC. Arsenic-trioxide-induced transcriptional activation of stress genes and expression of related proteins in human liver carcinoma cells ($HepG_2$). Cell Mol Biol. 2003; 49: 1070-1079.

84. Burns TF, El-Deiry WS. The p53 pathway and apoptosis. J Cell Physiol. 1999; 181: 231-239.

85. Martindale JL, Holbrook NJ. Cellular response to oxidative stress: signaling for suicide and survival. J Cell Physiol. 2002; 192: 1-15.

86. Yedjou CG, Tchounwou PB. Modulation of p53, c-fos, RARE, cyclin A, and cyclin D1 expression in human leukemia (HL-60) cells exposed to arsenic trioxide. Mol Cell Biochem. 2009; 331: 207-214.

87. Kim YJ, Chung JY, Lee SG, Kim JY, Park JE, Kim WR, et al. Arsenic trioxide-induced apoptosis in TM4 Sertoli cells: The potential involvement of p21 expression and p53 phosphorylation. Toxicology. 2011; 285: 142-151.

88. Lu TH, Su CC, Chen YW, Yang CY, Wu CC, Hung DZ, et al. Arsenic induces pancreatic β-cell apoptosis via the oxidative stress-regulated

mitochondria-dependent and endoplasmic reticulum stress-triggered signaling pathways. Toxicology Letters. 2011; 201: 15-26.

89. Salazar AM, Calderon-Aranda E, Cebrian ME, Sordo M, Bendesky A, Gómez-Muñoz A, et al. p53 Expression in circulating lymphocytes of non-melanoma skin cancer patients from an arsenic contaminated region in Mexico. A pilot study. Mol Cell Biochem. 2004; 255: 25-31.

90. Filippova M, Duerksen-Hughes PJ. Inorganic and dimethylated arsenic species induce cellular p53. Chem Res Toxicol. 2003; 16: 423-431.

91. Kang S, Song J, Kang H, Kang J, Kim S, Kang H, et al. Arsenic trioxide-induced apoptosis is independent of stress-responsive signaling pathways but sensitive to inhibition of inducible nitric oxide synthase in HepG2 cells. Exp and Mol Med. 2003; 35: 83-90.

92. Yih LH, Lee TC. Arsenite induces p53 accumulation through an ATM-dependent pathway in human fibroblasts. Cancer Res. 2000; 60: 6346-6352.

93. Chen F, Shi X. Intracellular signal transduction of cells in response to carcinogenic metals. Crit Rev OncolHematol. 2002; 42: 105-121.

94. Burnichon V, Jean S, Bellon L, Maraninchi M, Bideau C, Orsière T, et al. Patterns of gene expressions induced by arsenic trioxide in cultured human fibroblasts. Toxicol Lett. 2003; 143: 155-162.

95. Kastan MB, Onyekwere O, Sidransky D, Vogelstein B, Craig RW. Participation of p53 protein in the cellular response to DNA damage. Cancer Res. 1991; 51: 6304-6311.

96. Miyashita T, Krajewski S, Krajewska M, Wang HG, Lin HK, Liebermann DA, et al. Tumor suppressor p53 is a regulator of bcl-2 and bax gene expression *in vitro* and *in vivo*. Oncogene. 1994; 9: 1799-1805.

97. Park WH, Cho YH, Jung CW, Park JO, Kim K, Im YH, et al. Arsenic trioxide inhibits the growth of A498 renal cell carcinoma cells via cell cycle arrest or apoptosis. Biochem Biophys Res Commun. 2003; 300: 230-235.

98. Li X, Ding X, Adrian TE. Arsenic Trioxide Induces Apoptosis in Pancreatic Cancer Cells via Changes in Cell Cycle, Caspase Activation, and GADD Expression. Pancreas. 2003; 27: 174-179.

99. Moll UM, Wolff S, Speidel D, Deppert W. Transcription-independent proapoptotic functions of p53. Curr Opin Cell Biol. 2005; 17: 631-636.

100. Erster S, Moll UM. Stress-induced p53 runs a transcription-independent death program. Biochem Biophys Res Commun. 2005; 331: 843-850.

101. Liu X, Kim C, Yang J, Jemmerson R, Wang X. Induction of apoptotic program in cell-free extracts: requirement for dATP and cytochrome c. Cell. 1996; 86: 147-157.

102. Salazar AM, Ostrosky-Wegman P, Menendez D, Miranda E, Garcia-Carranca A, E Rojas. Induction of p53 protein expression by sodium arsenite. Mutat Res. 1997; 381: 259-265.

103. Schmidt CM, Cheng CN, Marino A, Konsoula R, Barile FA. Hormesis effect of trace metals on cultured normal and immortal human mammary cells. Toxicol Ind Health. 2004; 20: 57-68.

104. Bae DS, Gennings C, Carter WH Jr, Yang RS, Campain JA. Toxicological interactions among arsenic, cadmium, chromium, and lead in human keratinocytes.Toxicol Sci. 2001; 63: 132-142.

105. Raja WK, Satti J, Liu G, Castracane J. Dose Response of MTLn3 Cells to Serial Dilutions of Arsenic Trioxide and Ionizing Radiation. Dose Response. 2013; 11: 29-40.

106. Snow ET, Sykora P, Durham TR, Klein CB. Arsenic, mode of action at biologically plausible low doses: what are the implications for low dose cancer risk?. Toxicol Appl Pharmacol. 2005; 207: 557-564.

107. Ai Z, Lu W, Qin X. Arsenic trioxide induces gallbladder carcinoma cell apoptosis via downregulation of Bcl-2. Biochem Biophys Res Commun. 2006; 348: 1075-1081.

108. Chen GQ, Zhu J, Shi XG, Ni JH, Zhong HJ, Si GY, et al. In vitro studies on cellular and molecular mechanisms of arsenic trioxide (As2O3) in the treatment of acute promyelocytic leukemia: As2O3 induces NB4 cell apoptosis with downregulation of Bcl-2 expression and modulation of PML-RAR alpha/PML proteins. Blood. 1996; 88: 1052-1061.

109. Hirata H, Takahashi A, Kobayashi S, Yonehara S, Sawai H, Okazaki T, et al. Caspases are activated in a branched protease cascade and control distinct downstream processes in Fas-induced apoptosis. J Exp Med. 1998; 187: 587–600.

110. Li X, Ding X, Adrian TE. Arsenic Trioxide Induces Apoptosis in Pancreatic Cancer Cells via Changes in Cell Cycle, Caspase Activation, and GADD Expression. Pancreas. 2003; 27: 174-179.

111. Sen N, Das BB, Ganguly A, Mukherjee T, Tripathi G, Bandyopadhay S, et al. Campothecin induced mitochondrial dysfunction leading to programmed cell death in unicellular hemoflagellate Leishmania donovani. Cell Death Differ. 2004; 11: 924-936.

112. Bustamante J, Nutt L, Orrenius S, Gogvadze V. Arsenic stimulates release of cytochrome c from isolated mitochondria via induction of mitochondrial permeability transition. Review Article Toxicology and Applied Pharmacology. 2005; 207: 110-116.

Cite this article

Dugo EB, Yedjou CG, Stevens JJ, Tchounwou PB (2017) Therapeutic Potential of Arsenic Trioxide (ATO) in Treatment of Hepatocellular Carcinoma: Role of Oxidative Stress in ATO-Induced Apoptosis. Ann Clin Pathol 5(1): 1101.